Regulation of Transcriptional Activators by DNA-Binding Domain Ubiquitination

Regulation of Transcriptional Activators by DNA-Binding Domain Ubiquitination

Vivien Landré[1], Bhindu Revi[1], Maria Gil Mir[1], Chandra Verma[3], Ted R Hupp[1], Nick Gilbert[2] and Kathryn L Ball[1]

[1]Cell Signalling Unit, ECRC, IGMM and [2]MRC Human Genetics Unit MRC, IGMM, University of Edinburgh, Edinburgh EH4 2XR, UK.

[3]Bioinformatics Institute (A*STAR), 30 Biopolis Street, 07-01 Matrix, Singapore 138671; Department of Biological Sciences, National University of Singapore, 14 Science Drive 4, Singapore 117543; School of Biological Sciences, Nanyang Technological University, 60 Nanyang Drive, Singapore 637551, Singapore.

Corresponding Author: Kathryn L Ball, IGMM Edinburgh Cancer Research Centre University of Edinburgh, Western General Hospital, Crewe Road South, EH4 2XR UK. Phone: +44 (0) 131 651 8500, Fax: +44 (0) 131 651 8800, E-mail: Kathryn.Ball@igmm.ed.ac.uk.

Running title: DBD ubiquitination increases TA function

Keywords: p53, ubiquitination, post-translational modification, transcription, MDM2

Abstract

Ubiquitin is a key component of the regulatory network that maintains gene expression in eukaryotes, yet the molecular mechanism(s) by which non-degradative ubiquitination modulates transcriptional activator (TA) function is unknown. Here endogenous p53, a stress activated transcription factor required to maintain health, is stably monoubiquitinated, following pathway activation by IR or Nutlin-3, and localised to the nucleus where it becomes tightly associated with chromatin. Comparative structure-function analysis and *in silico* modelling demonstrate a direct role for DNA-binding domain (DBD) monoubiquitination in TA activation. When attached to the DBD of either p53, or a second TA IRF-1, ubiquitin is orientated towards, and makes contact with, the DNA. The contact is made between a predominantly cationic surface on ubiquitin and the anionic DNA. Our data demonstrates an unexpected role for ubiquitin in the mechanism of TA activity enhancement and provides insight into a new level of transcriptional regulation.

Introduction

Controlling the rate at which individual genes are expressed is fundamental to development, homeostasis and healthy ageing in eukaryotes. Underpinning the core transcriptional machinery is a complex network of transcriptional activators (TAs) that ensure tight regulation of gene expression[1, 2]. It has become clear that ubiquitin and the proteasome are key players in the regulatory network that maintains transcriptional control[3, 4, 5]. Yet, whilst there is a strong link between the rate at which TAs are degraded and their ability to drive expression from target promoters, the molecular mechanisms by which ubiquitin can activate transcription are poorly understood.

The role of the UPS in the regulation of p53, a well characterised transcription factor and tumour suppressor protein, has been studied extensively[6, 7, 8]. However, there is a paucity of studies linking site-specific ubiquitination to physiological outcome. In part this is because p53 displays a complex pattern of potential ubiquitin acceptor sites[9, 10]. Although ubiquitination has generally been linked to the negative regulation of p53, studies on the activated endogenous p53-pathway[11, 12] and on E4F1-mediated modification of p53[13] suggest that ubiquitination may be involved in upregulating this TA under some cellular conditions. MDM2 is the major, and best characterised, E3-ligase for p53. Under some conditions MDM2 can catalyses polyubiquination, as well as, p53 mono-ubiquitination[14] and this depends on the recruitment of E4-ligases such as, UBE4B-ligase[15] or MDM4[16].

Here the monoubiquitination of p53 is linked to its nuclear localisation and chromatin binding activity. Strikingly, in cells where the p53-pathway has been activated, polyubiquitination is switched to stable p53-monoubiquitination. Using comparative structure/function analysis in combination with *in silico* modelling and cell-based transcription assays, we demonstrate that modification at DBD Lys residues with monoubiquitin is sufficient to support TA function through a direct effect on DNA-binding activity.

Results

Nutlin and IR induce stable monoubiquitination of p53

The role of p53 in tumour suppression is closely linked with its sequence-specific DNA-binding activity and transactivation of genes required for growth control and cellular homeostasis. Intense efforts have therefore focused on activating p53 as a potential therapeutic avenue. Nutlin, for example, is a *cis*-imidazoline analogue, which binds to the MDM2 hydrophobic pocket[17] (Fig 1A) inhibiting its transrepressor function[18] but not its ability to ubiquitinate p53[12]. Consistent with Nutlin being an allosteric activator of MDM2 E3-activity, we have previously noted that Nutlin-mediated activation of p53, exemplified here by induction of the downstream targets $p21^{WAF1}$ and MDM2 (Fig 1B), is accompanied by the production of high molecular weight forms of p53[12, 18]. To establish whether these high molecular weight forms of p53 (Fig 1C) represented ubiquitin adducts, the ubiquitinated proteome was isolated from cells expressing His-ubiquitin (Fig 1D). When the His-ubiquitin modified proteins were analysed the profile of endogenous polyubiquitinated-p53 present in control cells (Lane 2) was striking altered by Nutlin-3 (Lane 3). Specifically, Nutlin-3 significantly enhanced (multi-) monoubiquitination of p53 and there was a loss of polyubiquitination. Thus, in control cells p53 is subject to polyubiquitination, consistent with its short half-life and proteasome mediated degradation[19]; whereas in Nutlin-3 treated cells p53 is predominantly monoubiquitinated leading us to speculate that Nutlin-3 mediated ubiquitination may play a role in regulating p53 activity rather than degradation. Notably, after Nutlin-3 treatment unmodified p53 was isolated together with the monoubiquitinated protein (Fig 1D, lane 3), this is in line with our observation that monoubiquitinated p53 can form mixed tetramers with unmodified p53 (unpublished data).

Based on previous studies[11] showing exposure of cells to IR increased p53 ubiquitination we investigated if IR, like Nutlin-3, led to enhanced monoubiquitination of p53. In agreement with Maki and Howley, (1997)[11] we found that IR produced a substantial change in His-ubiquitinated endogenous p53 (Fig 1E) with an increase in both mono- and poly-ubiquitination. The mixture of ubiquitin adducts likely reflects the fact that IR has a transient effect on the steady-state levels of p53[20], whereas the Nutlin-3 effect is longer lived[12]. However, by quantifying the first and second monoubiquitin bands (Fig 1E and 1F; Ub1 and Ub2) relative to the control samples (Fig 1E) we also found enrichment of monoubiquitinated p53 in IR treated cells. Thus, although Nutlin-3 produces a greater increase in monoubiquitinated p53, IR also reproducibly favours the generation of p53-monoubiquitin forms (Fig 1F).

It is unclear whether stable monoubiquitination in Nutlin or IR treated cells is linked to signalling events in the p53 activation pathway. We began to address this issue by determining whether Nutlin-3 and IR stimulated monoubiquitination was coupled to p53 degradation. p53 protein levels increased and, as expected for a short-lived protein, a portion of the TA accumulated in an ubiquitinated form when the proteasome was inhibited using lactacystin (Fig 1G). However, proteasome inhibition did not lead to the accumulation of Nutlin-3 or IR induced p53 forms; in fact there was a reproducible decrease in ubiquitinated p53 relative to the unmodified protein in cells treated with either agent plus lactacystin (Fig 1G). This is consistent with findings that monoubiquitin is removed from substrates under conditions of proteotoxic stress[21]. Further, whereas the basal half-life of p53 was approximately 20 min (Fig 1H), in Nutlin-3 or IR treated cells the $t_{0.5}$ increased to >

90 min (Fig 1H). These two experiments indicate that enhanced modification of p53 following pathway activation does not signal degradation. Further, when the turnover of the ubiquitinated p53 forms was monitored in control cells they had a short half-life of <15 min (Fig 1I; Ub-p53) consistent with these being rapidly degraded K48-polyubiquitinated p53-intermediates. Strikingly, the mono- and multi-monoubiquitinated forms of p53 detected in the presence of Nutlin-3 were not subject to turnover but were stable over 90 min (Fig 1I, S1A; Nutlin-3). Consistent with a mixed population of mono- and polyubiquitinated p53 (Fig 1E) the higher molecular weight forms in IR exposed cells were turned-over whereas the monoubiquitin-adducts persisted.

We next addressed the involvement of MDM2 in Nutlin stimulated p53 modification. First, we confirmed that whilst Nutlin-3 inhibits the high affinity interaction between MDM2 and the Box-I domain of p53, it stabilizes binding of MDM2 to a weaker interaction site (Box-V) in the core-domain (Fig 1J) that is essential for MDM2-mediated ubiquitination of p53[12]. Furthermore, Nutlin-3 did not inhibit binding of endogenous p53 and MDM2 in cells. In fact, when p53 immuno-precipitates were analysed there was a large fold increase in the amount of MDM2 found in complex with p53 (~20-fold) in the presence of the drug; whereas the amount of p53 protein in the immune complex was modestly increased (Fig 1K). To extend the immune-precipitation data proximity ligation assays (PLA; Fig 1L) were used to measure endogenous p53:MDM2 interactions *in situ*. Figure 1L (left-panel) shows a low level of p53:MDM2 complexes in untreated cells with PLA-foci distributed throughout the cell. However, in the presence of Nutlin-3 there was a significant increase in complex formation (Fig 1L; right bottom panel) and this was primarily in the nucleus. To determine whether the

increase in p53:MDM2 complex formation detected could result in MDM2-mediated ubiquitination of p53 we employed the MDM2 inhibitor protein ARF[22]. ARF was chosen as a tool rather than MDM2 knock-down using siRNA because we were unable to prevent significant increases in MDM2 protein levels in response to Nutlin-3 under conditions where a 60-70% knock-down was achieved in control cells (data not shown). In two different cell lines (Fig 1M), a titration of ARF could overcome the effect of Nutlin-3 on p53 ubiquitination. Studies showing that MDM2 is primarily a monoubiquitin ligase for p53[16], together with the data in Figures 1M and 1L, is consistent with the hypothesis that Nutlin-3 enhances p53 monoubiquitination through a process that involves MDM2.

Monoubiquitinated p53 is in the nucleus

Monoubiquitination has previously been proposed to signal p53 nuclear export and TA inhibition[23 24]. However, such studies used C-terminal ubiquitin-fusions or overexpression systems. Here we found recapitulation of the p53-monoubiquitination-pathway and its regulation by Nutlin-3 using exogenous components to be problematic, most likely reflecting the finely balanced nature of the pathway. To study the localisation of the ubiquitinated forms of p53 we used PLA (PLA; Fig 2A, S3). When PLA assays were carried out in control cells there was a background level of ubiquitinated p53 localised predominantly to the cytoplasm (Fig 2B) and no signal was detected in the control (Fig 2B) or in p53 null HCT116 cells (Fig S2A). There was a 5-fold increase in the number of positive p53:ubiquitin foci detected in the nucleus following Nutlin-3 treatment (Fig 2B, 2C and S3). In contrast, treatment with lactacystin induced PLA-foci throughout the cells (Fig S2B).

Data showing that monoubiquitinated p53 is located in the nucleus supports the hypothesis that it represents a step in the p53-activation pathway and suggests that the site-specific context of the ubiquitin-modification is likely to be a critical determinant of outcome.

A pool of monoubiquitinated p53 is tightly associated with the chromatin

We do not know if the nuclear pool of monoubiquitinated p53 is active for DNA-binding. To address this the nucleus was separated into soluble and chromatin bound fractions. Figure 3 shows in Nutlin-treated cells a minor portion of the total ubiquitinated p53 (Fig 3A) was recovered in the cytoplasm (Fig 3B). However, when we analysed the two nuclear fractions the majority of ubiquitinated p53 was chromatin-bound and ubiquitinated forms were below the level of detection in the soluble nuclear fraction. Whereas p53 protein levels were increased by Nutlin, HP1α, a nuclear marker, was consistently decreased in the soluble nuclear fraction of drug-treated cells. PARP, a marker for the soluble nuclear proteins, was unaffected by Nutlin-3 and Histone H3, a marker for the chromatin bound fraction, showed a small but consistent increase in drug-treated cells. To confirm that the high molecular weight forms of p53 detected in the chromatin bound fraction were generated by ubiquitination hypotonic lysis was used to isolate chromatin bound proteins (together with other insoluble proteins). The resultant pellet, which contained all the detectable DNA (Fig 3C) and the majority of histone H1, was resuspended and incubated with the p53-deubiquitinating enzyme HAUSP. Under these conditions monoubiquitinated p53 could be reduced to a single non-ubiquitinated form of the protein (Fig 3D). Thus, the nuclear pool of

modified-p53 detected by PLA (Fig 2) appears to be chromatin-bound and can be deubiquitinated.

Next a sucrose gradient sedimentation technique[25] was adapted to determine the distribution of p53 in relation to the density of the chromatin. Nuclei isolated from control, Nutlin-3 and IR treated cells were digested with micrococcal nuclease and analysed using an isokinetic 10/50% sucrose-density-gradient (Fig 3E). The top 1-3 fractions of the gradient contain the chromatin-unbound nuclear protein and is where recombinant p53 sediments (Fig S4A), fractions 4-6 contain loosely chromatin-associated proteins whereas tightly chromatin-associated proteins are present in fractions 7-9[25, 26] (Fig 3F). Analysis of IR (Fig 3G) or Nutlin-3 (Fig 3H) treated cells showed no pronounced shift in the distribution of total p53 compared to control cells, however, there was a striking appearance of mono- and multi-monoubiquitinated forms in the tightly chromatin-associated fractions. The data indicate that the (multi-)monoubiquitinated pool of p53 is in an active tightly chromatin-associated state. Note the chromatin fractionation is carried out under non-denaturing conditions and the pan de-ubiquitinase inhibitor NEM cannot be used (NEM inhibits p53 DNA-binding; Fig S4B); therefore the portion of p53 in a monoubiquitinated form is likely to be an underestimate.

A direct effect for p53 ubiquitination on its DNA-binding activity

p53 tetramers, purified from insect cells, can be separated into DNA-binding latent or activate fractions[27]. The DNA-binding active fraction of p53 was used to determine the effect of ubiquitin on binding to short oligonucleotide probes (Fig 4B, S5). p53 was

ubiquitinated *in vitro* by MDM2 or incubated in control reactions (Fig 4A). Though MDM2 is published to be a monoubiquitin ligase[14] we used mutant Ub (NoK; Lys residues are mutated to Arg) to ensure that no polyubiquitination of p53 took place (Fig 4A,B). The ability of p53 to bind a 33 bp element from the $p21^{WAF1}$ promoter was increased approximately 3-fold by ubiquitination and monoubiquitination was sufficient to stimulate activity. In addition ubiquitin had to be covalently attached to the TA as no enhancement was seen in control reactions containing ubiquitin and other assay components but no ATP (Fig 4B). To determine whether the effect of ubiquitination on p53 activity was specific to the $p21^{WAF1}$ promoter probes with the p53 responsive elements from *BAX, MDM2 and PUMA* were used (Fig 4C). Figure 4C shows that increased DNA-binding for ubiquitinated p53 was seen in all cases (3-4 fold). Using a rapid filter method we developed a quantitative stopped DNA-binding assay for p53 on a longer 66 bp fragment[28] (Fig 4D). Using conditions where there was a linear relationship between the amount of p53 and the amount of labelled DNA bound (Fig 4E), we observed that ubiquitination strongly enhanced binding of p53 to the longer fragment (Fig 4F). Thus, ubiquitination enhanced p53 activity on both short oligonucleotide and longer DNA fragments.

DBD ubiquitination can contribute directly to p53:DNA binding

Following pathway activation, stably monoubiquitinated p53 is in the nucleus where it is tightly associated with chromatin; furthermore ubiquitination directly enhances the interaction of p53 with DNA (Fig 3 and 4). Next we addressed the mechanism by which ubiquitin affects p53 binding to DNA. We hypothesised that ubiquitin-acceptor lysine residues located in the DBD of p53[10] were of most interest and in order to predict the

impact of monoubiquitination on p53:DNA-binding we used *in silico* modelling. First, a model in which Lys^{292} or Lys^{164} was modified by the C-terminal glycine of ubiquitin was generated using the human p53 DBD (PDB:1TUP) and ubiquitin (PDB: 1UBQ) structures and the HADDOCK webserver (Fig S6 and S7). The resulting models provided a starting structure for molecular dynamic (MD) simulations in an explicit solvent system. During the simulation ubiquitin underwent conformational changes that brought it into close proximity with the DNA, stabilizing intermolecular interactions (Fig 5B; movie S1). Ubiquitin occupied a similar position in relation to the p53 DBD when attached at K164 or K292 (Fig S7), as only K292 is targeted by MDM2[8] we decided to focus on this site. Electrostatic surface analysis of the complex using APBS (Adaptive Poisson-Boltzmann Solver) in Pymol, shows that addition of ubiquitin to the DBD extended the positively charged surface area that forms the protein:DNA interface (Fig 5B). Additionally, analysis of the DNA surface buried by the protein increased 53% when the DBD was monoubiquitinated (Fig 5C). Further, when the simulations were used to calculate binding energies between DNA and the p53 DBD, a significant decrease in ΔGB of monoubiquitinated compared to unmodified p53 was predicted (Fig 5C).

The *in silico* experiments are intriguing as they suggest a novel role for monoubiquitin in direct promotion of stable TA:DNA interactions, where specific TA DBD:DNA interactions are enhanced by non-specific ubiquitin:DNA binding.

DBD ubiquitination directly increases the DNA-binding ability of the TA IRF-1

p53 has multiple ubiquitin acceptor sites and the isolated DBD is not a substrate for MDM2 making it difficult to separate DBD ubiquitination from other p53 ubiquitination events. To complement our studies on p53, we therefore used IRF-1, an interferon regulated TA that is ubiquitinated exclusively in its DBD[29] (Fig 6A). IRF-1 ubiquitination occurs at several DBD-sites in close proximity to the DNA leading to speculation that it might affect IRF-1 DNA-binding activity[29]. Following modification of IRF-1 with either wt or NoK ubiquitin (Fig 6B), there was a significant gain in TA DNA-binding (Fig 6C,D). Models of monoubiquitinated DBD were generated as for p53[35] and MD simulations show a similar increase in buried DNA surface and significant decrease in ΔGB (Fig 6E,F). Thus, studies on IRF-1 support the concept that DBD monoubiquitin is sufficient to increase TA sequence-specific DNA-binding activity.

Key DBD lysine residues are required for maximal TA activity in cells

If the increase in DNA-binding activity and enhanced chromatin association seen on monoubiquitination of p53 result in a gain of TA function we would expect that loss of key acceptor Lys residues would adversely affect the TA activity of p53 and IRF-1. A series of conservative mutations (Lys to Arg) were introduced at known ubiquitin acceptor residues within, or adjacent to, the DBDs of p53 and IRF-1 (Fig 5A, 6A). First the activity of a p53 mutant in which four DBD ubiquitin acceptor sites were mutated (4R) was compared with one where six C-terminal domain acceptor-sites were substituted (6R). Whereas the 6R retained wild-type p53 activity levels, 4R was essentially transcriptionally inactive (Fig 7A). To pinpoint which of the Arg substitutions contributed to the loss of function, individual point mutant proteins were examined (Fig 7B-D). In agreement with the computational

analysis the K292R-mutant consistently demonstrated the most significant decrease in activity though it retained the ability to bind DNA (Fig S8). Thus, the loss of transcriptional activity seen in the K292R-mutant supports the idea that post-translational modification at this site might be involved in regulating p53 TA function.

Interestingly, K164R displayed a significant reduction in TA activity using MDM2- or BAX-reporters, but not on the p21-reporter suggesting that there could be some promoter context specificity with respect to modification at a given DBD-site. When similar experiments were carried out using IRF-1 with point mutations at each of five potential ubiquitin acceptor residues, only the K78R mutation consistently produced a decrease in both the TA (Fig 7E) and repressor (Fig 7F) activity.

Discussion

Though recently we have gained a greater appreciation of how both nonproteolytic and proteolytic ubiquitin-pathways are employed to regulate gene expression, there remains a significant lack of insight into the molecular mechanisms by which non-proteolytic modification, particularly monoubiquitination, regulates TA function[4]. Here we explore why p53 activation by Nutlin-3 or IR is accompanied by increased ubiquitination[11, 12]. This apparent contradiction is resolved by demonstrating an unexpected function for ubiquitin as an enhancer of p53 activity through a direct contribution to the TA:DNA binding interface (Fig 7G).

Artificial systems have revealed that ubiquitination of LexA-VP16 can promote transcriptional activity and that the E3-ligase component can be circumvented by fusing ubiquitin to the N-terminus[30]. Several studies have demonstrated that ubiquitin-fusions of, for example, FOXO4 or TAT, can modulate TA activity in mammalian cells[31, 32]. Though ubiquitin-fusion protein studies have been instrumental in demonstrating a link between monoubiquitin and TA function we must be cautious in their interpretation as they are unlikely to provide effective tools to study the impact of site-specific modification. To illustrate this, fusion of ubiquitin to the C-terminal regulatory domain of p53 leads to its nuclear export[23, 24]. In contrast endogenous p53, monoubiquitinated in response to activating signals, accumulates in the nucleus (Fig 2) and binds chromatin (Fig 3). Thus, we need to develop alternative approaches to explore physiological responses in a site- and signal-specific context. Site specificity is exemplified by the coactivator SCR-3, which is monoubiquitinated at two sites close to an LXXLL coregulator signature motif[33]. Mutation of the Lys acceptor sites to Arg inhibits nuclear receptor binding to the LXXLL, whereas monoubiquitination stimulates SCR-3 function. Thus studies on context and site-specificity of ubiquitination are likely to provide greater access to a mechanistic understanding of how signals lead to changes in gene expression.

An elegant series of experiments focused on the yeast α2 provides one mechanism by which ubiquitin can modulate transcription. In this case ubiquitination aids in the disassembly of transcription complexes from active promoters, a process that appears to be essential for robust derepression of α2 target genes[34]. An alternative mechanism is proposed for GAL4 where monoubiquitination prevents it from being 'stripped' off the DNA by components of

the proteasome[35]. This observation led to the suggestion that monoubiquitin might 'clamp' GAL4 onto the chromatin[36].

We have provided evidence for a novel interaction mode where ubiquitination at specific DBD Lys residues brings the charged surface of ubiquitin into a position where it can contribute directly to TA-activity by expanding the DNA-binding interface; this results in an increased buried DBD:DNA surface and a decrease in free energy for the interaction (Fig 5 and 6). Thus weak non-covalent ubiquitin interactions with DNA may act as a 'clutch' to enhance promoter residency and productive promoter output rather than rapid turnover or 'treadmilling' of TAs[37]. Alternatively, monoubiquitination may favour one mode of p53:DNA binding over another. Recent studies suggested that efficient function of p53 requires at least two modes of operation; a *search mode* mediated by the C-terminal domain that is characterized by largely nonspecific DNA binding coupled to fast-sliding, and a *recognition mode* in which p53 binds in a sequence-specific manner and can 'hop' on and off the DNA but is unable to slide [38].

The data presented here suggest that p53 can be regulated by ubiquitination in a manner that requires ubiquitin to play a direct role in DNA-binding. This model is supported by data showing that ubiquitin can bind weakly to DNA in its unconjugated state[39]. Further, our model would leave the hydrophobic binding face of ubiquitin[40] available for the potential recruitment of additional factors to further stabilise the TA:chromatin complex. In conclusion, site-specific monoubiquitination may impact on both the localization and function of p53.

Experimental Procedures

Cell culture, transfection, half-life determination, reporter assays and immunoblotting

A375 and H1299 cells were maintained in DMEM and RPMI medium (Invitrogen, Carlsbad, CA, USA) supplemented with 5% (v/v) FBS (Biosera, Boussens, France), 1% (v/v) penicillin/streptomycin (Invitrogen), respectively and grown at 37°C with 10 or 5% CO_2, respectively. Cell lysis was performed as described previously [12]. At 80% confluence, cells were transfected using Attractene (Qiagen, Germantown, MD, USA) following the manufacturer's instructions. Reporter assays were carried out using the Dual Luciferase Reporter System from Promega (Madison, WI, USA) following the supplier's instructions. Half-life determination was carried out as published [41]. 4–12% NuPAGE gels in a Mops buffer system (Invitrogen), run with either SeeBlue® or Page Ruler Pre-Stained protein ladder (ThermoFisher Scientific, Waltham, MA, USA), were analysed by immunoblots as described previously [20].

Reagents, plasmids and protein preparation

Antibodies were, DO1 mAb and CM1 pAb (anti-p53; Moravian Biotechnology, Brno, Czech Republic), 4B2 mAb (anti-MDM2; Moravian Biotechnology), anti-ubiquitin mAb (Santa Cruz Biotechnology, Santa Cruz, CA, USA), anti-p21 mAb (Calbiochem, Darmstadt, Germany), anti-GAPDH mAb and anti-Histone 3 pAb and -Epcam pAb (Abcam, Cambridge, UK), anti-β-actin mAb (Sigma-Aldrich, St. Louis, MO, USA), anti-HSP90α (Enzo Life Sciences, Exeter, UK), anti-HP1α and –PARP mAb's (Millipore, Billerica, MA, USA) and anti-IRF-1mAb (BD Biosciences, San Jose, CA, USA). Secondary antibodies were from Dako (Glostrop, Denmark). Antibodies were used at the concentrations indicated by the supplier. IRF-1 and p53 mutants were

constructed using a QuikChange® site-directed mutagenesis kit (Stratagene, Agilent Technologies, La Jolla, CA, USA) with primers designed for a codon change from Lys to Arg (Sigma). GST–IRF- 1 and GST–MDM2 were purified using glutathione–Sepharose and the tag was removed using Prescission Protease following the manufacturer's instructions (GE Healthcare, Pittsburgh, PA, USA). His– CHIP and His–UbcH5 were purified using Ni-NTA agarose (Qiagen) following supplier's instructions. His-USP7 (HAUSP) was supplied by Boston Biochem (Cambridge, MA, USA). Untagged p53 purified from Sf9 cells was a gift from Dr Jennifer Fraser (University of Edinburgh).

Ubiquitination assay

In vitro ubiquitination assays were carried out using our published method [12], with 25-250 ng of substrate [p53 or GST–IRF-1] and up to 60 ng MDM2 or His-CHIP, as indicated. Reactions were incubated at 30°C for 10-45 min as indicated. *In cell* ubiquitination assays were carried out as published [12] using A375 cells without MG132 treatment.

Proximity ligation assay

Cells grown on glass cover slips to 50% confluency were treated (as indicated), fixed by addition of formaldehyde solution (4% (v/v) formaldehyde, 100 mM PIPES (pH), 25 mM EDTA, 1 mM $MgCl_2$) for 15 min and permeabilised using 1% Triton X-100 in PBS for 10 min. Duolink® II assays (Olink® Bioscience, Uppsala, Sweden) were carried out following the suppliers instructions. The fluorescent signal was imaged using an Axioplan2 (Zeiss, Göttingen, Germany) fluorescent microscope.

Fractionation of cells and chromatin

Nuclei isolation, digestion and lysis was carried out as previously described [25] all solutions were supplemented with 20 mM DTT. Soluble chromatin was fractionated using 10-50% (w/v) isokinetic sucrose gradients in TEEP80 (10 mM Tris-HCl, pH7.6, 0.1 mM EDTA, 0.1 mM EGTA, 2 mM pefabloc, 80mM NaCl, 20 mM DTT) by centrifugation for 110 min at 50 000 rpm and 4°C. Fractions (500 μl) were collected by upward displacement with continuous monitoring of the absorbance profile. Each fraction was analysed for protein content following ethanol precipitation, washing to remove all sucrose and resuspension in SDS-sample buffer. DNA was extracted from the fractions using phenol/chloroform and enriched by ethanol precipitation. DNA pellets were washed, re-suspended in H_2O and analysed on a 1% agarose gel. Subcellular Fractionations was carried out using a Subcellular Protein Fractionation kit (ThermoFisher) following supplier's instructions.

To fractionate cells into soluble and insoluble fractions for deubiquitination assays, cells were washed in ice-cold PBS, and lysed on the plate in gentle lysis buffer (PBS + 0.5% Triton-X 100, 5 mM EDTA, 20 mM DTT, 0.05 mM Pefabloc) for 20 minutes with shaking. Cells were harvested and centrifuged at 13000 rpm for 5 minutes. The Pellet was resuspended in deubiquitination buffer (50 mM Hepes pH 7.8, 50 mM NaCl, 1 mM EDTA, 10 mM DTT and 5% glycerol) and incubated for 30 min at 30^{o}C in the absence or presence of HAUSP (50 ng; Boston Biochem).

DNA-binding assays

Electrophoretic Mobility-Shift Assays (EMSAs) were carried out as described previously [27]. Briefly, indicated amounts of p53 were incubated with 40 ng of ^{32}P-labelled oligonucleotides for p21, BAX, and MDM2 promoter (see table S1 for details of oligonucleotides), in EMSA buffer [20 mM HEPES (pH 7.5), 50 mM KCl, 5% glycerol, 0.4 mM DTT, 0.1 mg/ml BSA, 0.05% Triton X-100, 0.125 mg/ml poly(dI- dC) and 0.04 mg/ml salmon sperm DNA] for 30 min at RT. Samples were analysed by PAGE (5% gel) and radiolabelled bands were detected using a Storm840 phosphoimager (GE Healthcare).

For Filter binding analysis, DNA binding assays (25 μl) contained 10 ng of a 5'-^{32}P-end-labeled 66 bp fragment from the p21WAF1 promoter and 10 fold molar excess of unlabeled salmon sperm DNA in buffer containing 25 mM HEPES-KOH (pH 7.8), 5 mM $MgCl_2$, 2 mM DTT, and 50 mM KCI. Following the addition of p53 (ubiquitinated or non-ubiquitinated), the samples were incubated at 25^{o}C for 30 min. Reactions were filtered through nitrocellulose filters (HAWP, 0.22 μm, 13 mm Millipore), washed with the above buffer (250 μl) and equilibrated at the incubation temperature. Radiolabeled DNA retained on the filters was quantified using a Storm840 phosphoimager (GE Healthcare).

For immobilized DNA-binding assays, microtiter plates were coated with streptavidin (1 μg/well in PBS) and incubated with biotin-tagged C1 oligonucleotide (60 pmol) for 1 h. Unbound oligonucleotide was removed by washing and non-reactive sites blocked using 3% (w/v) BSA in PBS. A titration of IRF-1 (unmodified or ubiquitinated) in 25 mM HEPES, pH 7.5, 50 mM KCl, 10 mM $MgCl_2$, 5% (v/v) glycerol, 0.1% (v/v) Tween-20 was added for 1 h. After washing, binding was detected using anti-IRF-1 mAb and electrochemical luminescence quantified using a luminometer (Labsystems, DYNEX Technology, Chantilly, VA, USA).

Generation of models using HADDOCK

Models of IRF-1 and p53 DBD conjugated to ubiquitin were generated using the HADDOCK webserver [42, 43] (as described previously[29]). The C-terminus of the p53 DBD crystal structure (PDB:1TUP, resolved at 2.2 Å[44]) was extended from residue 291 by grafting residue 292 from 2AHI (resolved at 1.85 Å, [45]) onto 1TUP. For the model, the C-terminal glycine residue of ubiquitin (Gly^{76}) was selected as the active residue on ubiquitin (PDB :1UBQ, resolved at 1.8 Å [40]) and Lys [292] on p53 or Lys^{78} on IRF-1 (PDB:1IF1, resolved at 3 Å [46]), was chosen as the active residue in the p53 or IRF-1 crystal structure, respectively. No passive residues were selected. From the output, the three best structures of the four clusters with the best HADDOCK score were used for analysis (see Fig S6). The models were produced in the absence of DNA and subsequently overlaid with the DBD complexed to DNA as seen in the crystal structure. Any complex exhibiting a major clash between the position of ubiquitin and DNA was discarded, and the remaining model was used as the starting structure for a 40 ns molecular dynamic (MD) simulation in an explicit solvent system. Electrostatic surface analysis of the IRF-1/p53 DBD:monoubiquitin complex were carried out using APBS (Adaptive Poisson-Boltzmann Solver [47]) in PyMOL v1.4.1 (http://www.pymol.org).

Molecular Dynamic Simulations

To model the interactions of DNA with p53 or IRF-1 in its ubiquitinated or unmodified forms, the (extended) crystal structures of the p53 DBD (PDB: 1TUP, 2AHI) or IRF-1 DBD (PDB: 1IF1) and the model of monoubiquitinated p53 or IRF-1 DBD in complex with DNA as generated above were used. The N- and C- termini of the p53 DBD were capped with acetyl (ACE) and N-methyl (NME) respectively to keep them neutral. Molecular dynamics simulations were

performed with the SANDER module of the AMBER (Assisted Model Building Refinement) 9 package (http://ambermd.org/) together with the ff99SB forcefield. The antechamber and LEaP modules were used to set up the simulation. Systems were solvated in a TIP3P water box with walls at least 8 Å away from any protein atom and net charges on the protein were neutralized using counter ions as required (20-26 Na^+). To simulate a covalent linkage, a distance restraint between Gly^{76} of ubiquitin and Lys^{292} of p53 or Lys^{78} of IRF-1 (between 1.2 and 2Å) was created using a DISANG file in AMBER. A brief energy minimization was carried out followed by heating of the systems to 300 K and subsequent MD simulations were performed under constant pressure (1 atm) and temperature (300 K) using the Sander module. Structures were stored every 2 ps as described before [48]. The free energies of binding (ΔG_{bind}) of the p53 DBD +/- ubiquitin to DNA were computed and visualizations were carried out as described earlier [48]. Figures were prepared using PyMOL.

Acknowledgements

VL was funded by a SULSA studentship, MGM by a CRUK Scottish Power alliance studentship both awarded to KLB. VL obtained a training award from the EACR to work for 3 months with CV. BR receives funding from Petplan. NG is an MRC Senior Fellow (MR/J00913X/1). We would like to thank Dr Maria Mativa for preparation of the pcDNA3.1 IRF-1 K to R mutants.

Conflict of Interest

There is no conflict of interest to declare.

Supplementary information is available at Cell Death and Differentiation's website.

References

1. Lemon B, Tjian R. Orchestrated response: a symphony of transcription factors for gene control. *Genes Dev* 2000, **14**(20)**:** 2551-2569.

2. Naar AM, Lemon BD, Tjian R. Transcriptional coactivator complexes. *Annu Rev Biochem* 2001, **70:** 475-501.

3. Ee G, Lehming N. How the Ubiquitin Proteasome System Regulates the Regulators of Transcription. *Transcription* 2012, **3**(5).

4. Geng F, Wenzel S, Tansey WP. Ubiquitin and proteasomes in transcription. *Annu Rev Biochem* 2012, **81:** 177-201.

5. Landre V, Rotblat B, Melino S, Bernassola F, Melino G. Screening for E3-ubiquitin ligase inhibitors: challenges and opportunities. *Oncotarget* 2014, **5**(18)**:** 7988-8013.

6. Brooks CL, Gu W. p53 regulation by ubiquitin. *FEBS Lett* 2011, **585**(18)**:** 2803-2809.

7. Hock A, Vousden KH. Regulation of the p53 pathway by ubiquitin and related proteins. *Int J Biochem Cell Biol* 2010, **42**(10)**:** 1618-1621.

8. Soussi T, Wiman KG. TP53: an oncogene in disguise. *Cell Death Differ* 2016 **22**(8)**:** 1239-1249.

9. Shloush J, Vlassov JE, Engson I, Duan S, Saridakis V, Dhe-Paganon S*, et al.* Structural and functional comparison of the RING domains of two p53 E3 ligases, Mdm2 and Pirh2. *The Journal of biological chemistry*, **286**(6)**:** 4796-4808.

10. Chan WM, Mak MC, Fung TK, Lau A, Siu WY, Poon RY. Ubiquitination of p53 at multiple sites in the DNA-binding domain. *Mol Cancer Res* 2006, **4**(1)**:** 15-25.

11. Maki CG, Howley PM. Ubiquitination of p53 and p21 is differentially affected by ionizing and UV radiation. *Mol Cell Biol* 1997, **17**(1)**:** 355-363.

12. Wallace M, Worrall E, Pettersson S, Hupp TR, Ball KL. Dual-site regulation of MDM2 E3-ubiquitin ligase activity. *Mol Cell* 2006, **23**(2)**:** 251-263.

13. Le Cam L, Linares LK, Paul C, Julien E, Lacroix M, Hatchi E*, et al.* E4F1 is an atypical ubiquitin ligase that modulates p53 effector functions independently of degradation. *Cell* 2006, **127**(4)**:** 775-788.

14. Lai Z, Ferry KV, Diamond MA, Wee KE, Kim YB, Ma J*, et al.* Human mdm2 mediates multiple mono-ubiquitination of p53 by a mechanism requiring enzyme isomerization. *J Biol Chem* 2001, **276**(33)**:** 31357-31367.

15. Wu H, Leng RP. UBE4B, a ubiquitin chain assembly factor, is required for MDM2-mediated p53 polyubiquitination and degradation. *Cell Cycle* 2011, **10**(12)**:** 1912-1915.

16. Wang X, Wang J, Jiang X. MdmX protein is essential for Mdm2 protein-mediated p53 polyubiquitination. *J Biol Chem* 2011, **286**(27)**:** 23725-23734.

17. Vassilev LT. Small-molecule antagonists of p53-MDM2 binding: research tools and potential therapeutics. *Cell cycle (Georgetown, Tex* 2004, **3**(4)**:** 419-421.

18. Wawrzynow B, Pettersson S, Zylicz A, Bramham J, Worrall E, Hupp TR*, et al.* A function for the RING finger domain in the allosteric control of MDM2 conformation and activity. *J Biol Chem* 2009, **284**(17)**:** 11517-11530.

19. Brooks CL, Gu W. p53 ubiquitination: Mdm2 and beyond. *Molecular cell* 2006, **21**(3)**:** 307-315.

20. Pamment J, Ramsay E, Kelleher M, Dornan D, Ball KL. Regulation of the IRF-1 tumour modifier during the response to genotoxic stress involves an ATM-dependent signalling pathway. *Oncogene* 2002, **21**(51)**:** 7776-7785.

21. Kim W, Bennett EJ, Huttlin EL, Guo A, Li J, Possemato A*, et al.* Systematic and quantitative assessment of the ubiquitin-modified proteome. *Molecular cell*, **44**(2)**:** 325-340.

22. Honda R, Tanaka H, Yasuda H. Oncoprotein MDM2 is a ubiquitin ligase E3 for tumor suppressor p53. *FEBS Lett* 1997, **420**(1)**:** 25-27.

23. Brooks CL, Li M, Gu W. Monoubiquitination: the signal for p53 nuclear export? *Cell cycle (Georgetown, Tex* 2004, **3**(4)**:** 436-438.

24. Carter S, Bischof O, Dejean A, Vousden KH. C-terminal modifications regulate MDM2 dissociation and nuclear export of p53. *Nature cell biology* 2007, **9**(4)**:** 428-435.

25. Gilbert N, Allan J. Distinctive higher-order chromatin structure at mammalian centromeres. *Proc Natl Acad Sci U S A* 2001, **98**(21)**:** 11949-11954.

26. Gilbert N, Thomson I, Boyle S, Allan J, Ramsahoye B, Bickmore WA. DNA methylation affects nuclear organization, histone modifications, and linker histone binding but not chromatin compaction. *J Cell Biol* 2007, **177**(3)**:** 401-411.

27. Hupp TR, Lane DP. Allosteric activation of latent p53 tetramers. *Curr Biol* 1994, **4**(10)**:** 865-875.

28. McKinney K, Mattia M, Gottifredi V, Prives C. p53 linear diffusion along DNA requires its C terminus. *Molecular cell* 2004, **16**(3)**:** 413-424.

29. Landre V, Pion E, Narayan V, Xirodimas DP, Ball KL. DNA-binding regulates site-specific ubiquitination of IRF-1. *Biochem J* 2013, **449**(3)**:** 707-717.

30. Salghetti SE, Caudy AA, Chenoweth JG, Tansey WP. Regulation of transcriptional activation domain function by ubiquitin. *Science* 2001, **293**(5535)**:** 1651-1653.

31. van der Horst A, de Vries-Smits AM, Brenkman AB, van Triest MH, van den Broek N, Colland F*, et al.* FOXO4 transcriptional activity is regulated by monoubiquitination and USP7/HAUSP. *Nat Cell Biol* 2006, **8**(10)**:** 1064-1073.

32. Bres V, Kiernan RE, Linares LK, Chable-Bessia C, Plechakova O, Treand C*, et al.* A non-proteolytic role for ubiquitin in Tat-mediated transactivation of the HIV-1 promoter. *Nat Cell Biol* 2003, **5**(8)**:** 754-761.

33. Wu RC, Feng Q, Lonard DM, O'Malley BW. SRC-3 coactivator functional lifetime is regulated by a phospho-dependent ubiquitin time clock. *Cell* 2007, **129**(6)**:** 1125-1140.

34. Wilcox AJ, Laney JD. A ubiquitin-selective AAA-ATPase mediates transcriptional switching by remodelling a repressor-promoter DNA complex. *Nat Cell Biol* 2009, **11**(12)**:** 1481-1486.

35. Archer CT, Delahodde A, Gonzalez F, Johnston SA, Kodadek T. Activation domain-dependent monoubiquitylation of Gal4 protein is essential for promoter binding in vivo. *J Biol Chem* 2008, **283**(18)**:** 12614-12623.

36. Geng F, Wenzel S, Tansey WP. Ubiquitin and proteasomes in transcription. *Annual review of biochemistry* 2012, **81:** 177-201.

37. Lickwar CR, Mueller F, Hanlon SE, McNally JG, Lieb JD. Genome-wide protein-DNA binding dynamics suggest a molecular clutch for transcription factor function. *Nature*, **484**(7393)**:** 251-255.

38. Tafvizi A, Huang F, Fersht AR, Mirny LA, van Oijen AM. A single-molecule characterization of p53 search on DNA. *Proceedings of the National Academy of Sciences of the United States of America*, **108**(2)**:** 563-568.

39. Cary PD, King DS, Crane-Robinson C, Bradbury EM, Rabbani A, Goodwin GH*, et al.* Structural studies on two high-mobility-group proteins from calf thymus, HMG-14 and HMG-20 (ubiquitin), and their interaction with DNA. *European journal of biochemistry / FEBS* 1980, **112**(3)**:** 577-580.

40. Vijay-Kumar S, Bugg CE, Cook WJ. Structure of ubiquitin refined at 1.8 A resolution. *J Mol Biol* 1987, **194**(3)**:** 531-544.

41. Pion E, Narayan V, Eckert M, Ball KL. Role of the IRF-1 enhancer domain in signalling polyubiquitination and degradation. *Cell Signal* 2009, **21**(10)**:** 1479-1487.

42. de Vries SJ, van Dijk AD, Krzeminski M, van Dijk M, Thureau A, Hsu V*, et al.* HADDOCK versus HADDOCK: new features and performance of HADDOCK2.0 on the CAPRI targets. *Proteins* 2007, **69**(4)**:** 726-733.

43. Dominguez C, Boelens R, Bonvin AM. HADDOCK: a protein-protein docking approach based on biochemical or biophysical information. *J Am Chem Soc* 2003, **125**(7)**:** 1731-1737.

44. Cho Y, Gorina S, Jeffrey PD, Pavletich NP. Crystal structure of a p53 tumor suppressor-DNA complex: understanding tumorigenic mutations. *Science* 1994, **265**(5170)**:** 346-355.

45. Kitayner M, Rozenberg H, Kessler N, Rabinovich D, Shaulov L, Haran TE*, et al.* Structural basis of DNA recognition by p53 tetramers. *Mol Cell* 2006, **22**(6)**:** 741-753.

46. Escalante CR, Yie J, Thanos D, Aggarwal AK. Structure of IRF-1 with bound DNA reveals determinants of interferon regulation. *Nature* 1998, **391**(6662)**:** 103-106.

47. Baker NA, Sept D, Joseph S, Holst MJ, McCammon JA. Electrostatics of nanosystems: application to microtubules and the ribosome. *Proc Natl Acad Sci U S A* 2001, **98**(18)**:** 10037-10041.

48. Joseph TL, Madhumalar A, Brown CJ, Lane DP, Verma CS. Differential binding of p53 and nutlin to MDM2 and MDMX: computational studies. *Cell Cycle* 2010, **9**(6)**:** 1167-1181.

49. Vassilev LT, Vu BT, Graves B, Carvajal D, Podlaski F, Filipovic Z*, et al.* In vivo activation of the p53 pathway by small-molecule antagonists of MDM2. *Science* 2004, **303**(5659)**:** 844-848.

50. Shloush J, Vlassov JE, Engson I, Duan S, Saridakis V, Dhe-Paganon S*, et al.* Structural and functional comparison of the RING domains of two p53 E3 ligases, Mdm2 and Pirh2. *J Biol Chem* 2011, **286**(6)**:** 4796-4808.

Figure legends

Figure 1. Nutlin and IR induce stable monoubiquitination of p53

(A) Nultin-2 (yellow sticks) bound to the hydrophobic pocket of MDM2 (shown as surface); PDB: 1RV1 [49].

(B) Immunoblot of A375 cells treated with Nutlin-3 (10 μM) or DMSO control for 8 h, lysed in Triton-X buffer and developed using indicated antibodies.

(C) Immunoblot of A375 cells treated with Nultin-3 (10 μM) for 0-8 h, lysed in urea buffer and developed using DO1 to detect endogenous p53.

(D + E) Immunoblot of His-ubiquitinated endogenous proteins isolated using Ni-NTA chromatography after A375 cells were transfected with His-ubiquitin (0.5 μg) for 20 h and treated with (D) Nutlin-3 (10 μM) or DMSO for the last 8 h, or (E) untreated (lane 2) or treated with either DMSO (lane 3), Nutlin-3 (10 μM, for last 8 h; lane 4) or IR (5 Gy, with a 3h recovery; lane 5). Cells were collected and lysed, the His-ubiquitinated proteome was isolated using Ni-NTA chromatography. The membrane was developed using antibodies to the indicated proteins. Cartoon in (D); polyubiquitination in control cells will lead to proteasomal degradation, whereas the role of monoubiquitination is unknown.

(F) Quantification of results from (E) using Image J. The fold increase of unmodified p53 and p53 attached to 1, 2 or 5 ubiquitins in respect to the control samples was calculated and is shown.

(G) Immunoblot of A375 cells treated with Nutlin-3 (10 μM), DMSO control or irradiated as above and simultaneously treated with lactacystin (10 μM) for 4 h, lysed in urea buffer and

developed using DO1. The IR samples were analysed on the same gel but lanes 3 and 4 were not adjacent (indicated by a line) to lanes 1 and 2.

(H + I) Immunoblot of A375 cells treated with Nutlin-3 (10 μM, 8 h; or DMSO control) or irradiated as in (D) and treated with cycloheximide (30 μg/ml) for the times indicated, lysed in (H) Triton-X buffer or (I) urea buffer and developed with DO1. The data from J was analysed by densitometry and depicted graphically.

(J) Immobilized p53 Box-I (PPLSQETFSDLWKLLP) and Box V (RNSFEVRVCACGRD) peptides incubated with MDM2 (100 ng) and a titration of Nutlin-3 (0-8 μM). Binding was detected using an anti-MDM2 mAb.

(K) Immunoblot of p53 mAb immunoprecipitate from A375 cell lysate after Nutlin-3 (10 μM) or DMSO treatment for 8 h.

(L) Left panel: PLA in A375 cells treated with Nultin-3 (10 μM) for 8 h developed using anti-MDM2 mAb 4B2 and p53 pAb CM1 or BSA control. The data is representative of 4 separate experiments. Right top panel: Cartoon of the PLA reaction where antibodies binding to MDM2 and p53 are detected by secondary antibodies conjugated to complementary DNA that come together to form a rolling circle PCR template (detected using fluorescent probes) when the two proteins are closer than 40 nm. Right lower panel: PLA foci in at least 10 fields were counted; the average numbers of foci/cell are shown. The P value ** was < 0.01. The P value was calculated using Student's t-test.

(M) A375 cells were transfected with a titration of p19ARF or empty vector (DNA normalised using empty vector). After 24h the cells were treated with Nutlin or DMSO alone (as above) and harvested 4h later into urea lysis buffer. The lysates were analysed by immunoblot developed using antibodies to the proteins indicated. (C=control).

All experiments represent the results of at least 3 independent experiments.

Figure 2. Monoubiquitinated endogenous p53 localizes to the nucleus

(A) Schematic illustration of the PLA as in figure 3.

(B) PLA in A375 cells treated with Nultin-3 (10 μM) for 8 h using anti-ubiquitin only, or anti-ubiquitin and p53 DO1 as indicated.

(C) PLA foci in at least 100 cells were counted; the average numbers of foci/cell are shown. The P value was calculated using Student's t-test.

Figure 3. A pool of monoubiquitinated p53 is tightly associated with the chromatin

(A) Duplicate plates of A375 cells were treated with carrier (DMSO) or Nutlin-3 (10 μM) for 8 h prior to harvesting and lysed in urea lysis buffer. The whole cell lysates were analysed using SDS-PAGE followed by immunoblot developed using anti-p53 mAb DO-1.

(B) A375 cells were prepared as in (A) and fractionated using a Subcellular Protein Fractionation kit into cytoplasmic (Cy), membrane (M), chromatin bound (CB), soluble nuclear (SN) and cytoskeletal (Cs) fractions. The fractions were analysed by SDS-PAGE and immunoblot; proteins were detected using antibodies to the indicated proteins. The black lines mean that the samples were analysed at the same time and immunoblotted together but were not adjacent on the gel. Where there is a gap samples were analysed using the same equipment but on separate gels (in this case markers were used to ensure normalisation of electrophoresis and transfer). The data are representative of duplicates from 2 separate experiments.

(C) Cells were lysed under hypotonic conditions and the insoluble and soluble fractions collected. DNA content was determined using chloroform-methanol extraction and analysed on an agarose gel, whereas protein was analysed by SDS-PAGE/immunoblot and histone H1 detection.

(D) Irradiated cells (5 Gy) were lysed to isolate insoluble proteins as in (C). The pellet was resuspended and incubated in the present or absence of HAUSP for 30 min at 30^{o}C prior to analysis by SDS-PAGE/immunoblot and detection of p53 using DO-1. Unmodified (p53) and ubiquitinated p53 (p53-Ub) are indicated.

(E) Experimental outline of nuclei fractionation using sucrose gradient centrifugation. A375 cell nuclei were isolated, RNA removed and chromosomal DNA partially digested using micrococcal nuclease. Separation was performed using a 10-50% sucrose gradient and fractions (0.5 ml) collected for analysis. A UV trace and agarose gel of the DNA content are shown, plus an immunoblot for histones.

(F) Schematic illustration of distribution of chromatin and chromatin associated protein in the sucrose gradient.

(G + H) Nuclei of control or irradiated (G; 5 Gy, 3h recovery) and Nutlin-3 (H; 10 μM for 8 h) treated A375 cells fractionated as described in (E) and analysed by immunoblot using DO1 and Histone H3 antibodies. The data are representative of at least two individual experiments.

Figure 4. DBD ubiquitination can contribute directly to p53:DNA binding

(A) p53 was ubiquitinated for 45 min with either wt or mutant ubiquitin (NoK).

(B) Binding of modified p53 (500 ng) (from A) to p21-oligonucleotides was measured in an EMSA. Where indicated DO1 was added to supershift the p53:DNA complex. The control was p53 incubated in the ubiquitination reaction plus AMP in place of ATP to prevent ubiquitination. Bands were quantified using Image J and are presented graphically (B, right panel).

(C) As in (B) except that a range of p53 binding oligonucleotides based on the indicated promoters were used. The control reactions (p53) were incubated in the ubiquitination reaction plus AMP in place of ATP to prevent ubiquitination.

Results in are representative of at least 2 independent experiments.

(D) Nucleotide sequence of the DNA fragment used to assay p53 DNA-binding. The p53 binding element is shown in blue/red.

(E) p53 (purified from Sf21 cells) binding to the radiolabelled probe shown in D was determined using a filter binding assay. The graph shows fmols of DNA bound per ng of p53.

(F) Immunoblot p53 (detected using DO-1) ubiquitinated by MDM2 in the presence or absence of ATP incubated for either 15 or 60 min (left panel). p53 from the ubiquitination reactions shown was subsequently assayed for DNA binding as in E (right panel). The results are indicative of 3 separate experiments.

Figure 5. MD simulations are supported by increases in p53 DNA-binding activity

(A) Domain and crystal structure (DBD only, pdb:1TUP) of p53 with Lys that are subject to ubiquitination by MDM2 (red) and/or Pirh2 indicated [50]

(B) Model of the p53:ubiquitin:DNA complex. Electrostatic surface analysis of the ubiquitin:TA model used the APBS Pymol plugin. Blue indicates regions of positive potential, while red indicates regions of negative potential.

(C) The DNA surface buried by the p53-1DBD alone or in complex with ubiquitin was calculated using Pymol (upper panel). Molecular Dynamic Simulations were carried out on the complex of p53 DBD:DNA (PDB:1TUP) and the p53 DBD:DNA:ubiquitin model. The simulations were used to compute the free binding free energy (in kcal/mol) of DNA with p53 DBD +/- ubiquitin (lower panel).

Figure 6. DBD ubiquitination directly increases the DNA binding ability of the TA IRF-1

(A) Domain and crystal structure of IRF-1 (DBD only, pdb: 1IF1) with Lys that are subject to ubiquitination indicated.

(B) *In vitro* ubiquitination reactions with CHIP, IRF-1 plus wt or mutant (NoK) ubiquitin were incubated for 45 min. The control was IRF-1 incubated in the ubiquitination reaction plus AMP in place of ATP to prevent ubiquitination.

(C) Binding of IRF-1 (from B) to C1 oligonucleotide probe in an EMSA (100 ng IRF-1/lane), bands were quantified using Image J and are presented graphically (lower panel).

(D) Binding of IRF-1 (from B) to C1 oligonucleotide immobilized on a microtiter well incubated with increasing amounts of IRF-1 (0-40 ng, from B) in the mobile phase. Binding was detected using anti-IRF-1 mAb. Results shown are representative of 3 independent experiments.

(E) Model of the IRF-1:ubiquitin:DNA generated by superimposing IRF-1:ubiquitin onto the IRF-1DBD:DNA crystal structure. Electrostatic surface analysis of the ubiquitin:TA model

used the APBS Pymol plugin. Blue indicates positive charge, while red shows negative charge.

(F) The DNA surface buried (upper panel) by the IRF-1DBD alone or in complex with ubiquitin and the free binding energy (lower panel) were calculated as in 5C and are shown

Figure 7. Mutation of the ubiquitin acceptor lysines in p53 and IRF-1 DBD decrease their transcriptional activity

(A) H1299 cells were transfected with wt or Lys→Arg mutant p53 constructs (100 ng) plus p21-Luc (140 ng) and control Renilla-Luc (60 ng). 6R has all 6 C-terminal ubiquitination sites mutated and 4R has all 4 ubiquitination sites in or proximal to the DBD mutated. Post transfection (24 h), cells were harvested and dual luciferase reporter assays performed. Results were normalised by expressing firefly/renilla luciferase activity in relative light units (RLU) as the mean +/- S.D. Cell lysates were analysed by SDS-PAGE/Immunoblot.

(B-D) H1299 cells were transfected with either wt or mutant p53 (Lys→Arg point mutations at Lys^{101}, Lys^{164}, Lys^{292}, Lys^{305} or 4R) and assayed as in (A) with luciferase reporter plasmids for p21 (B), MDM2 (C) or Bax (D).

(E+F) H1299 cells were transfected with wt or Lys→Arg mutant IRF-1 constructs (100 ng) for Lys^{39}, Lys^{50}, Lys^{78}, Lys^{95} or Lys^{117} and assayed as above with luciferase reporters for TRAIL (E) or CDK (F)

(G) Model of a novel role of monoubiquitination in the activation of transcription.

Figure 1

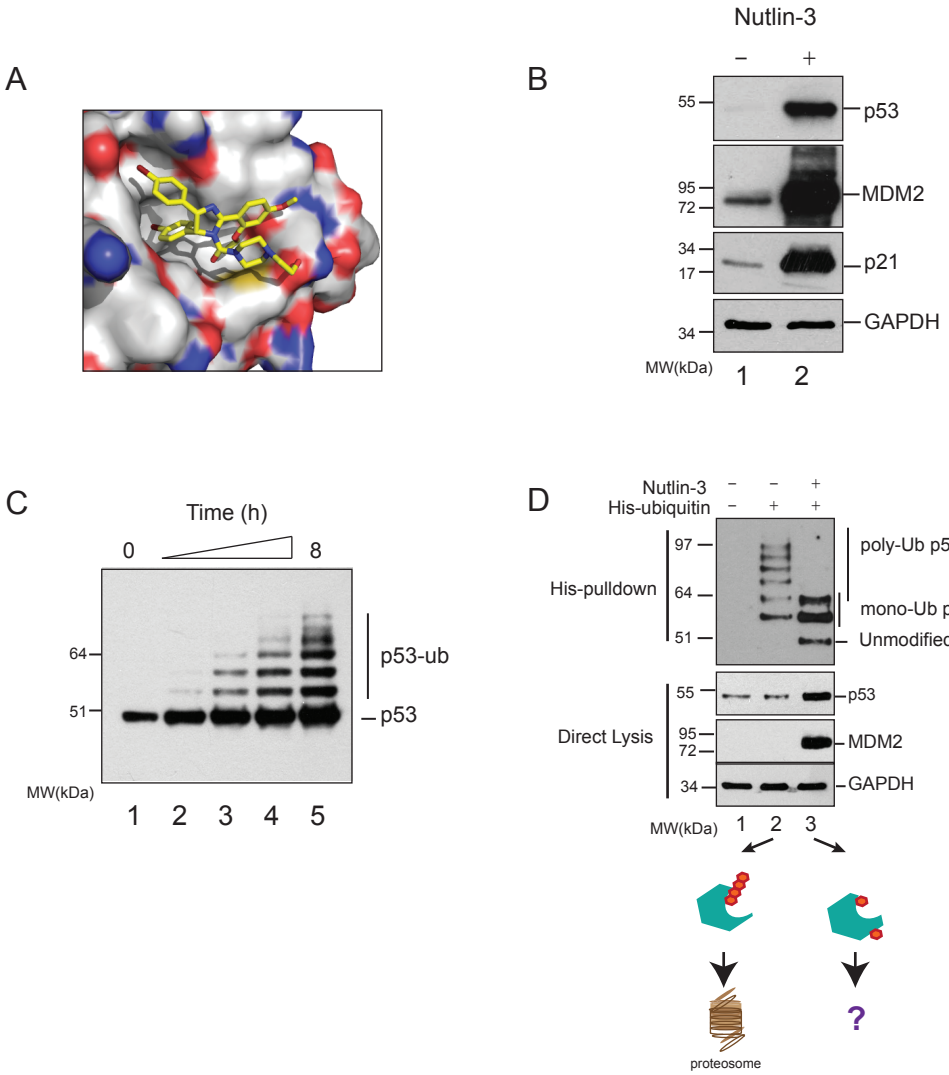
A
B
Nutlin-3
–
+
55
p53
95
72
MDM2
34
17
p21
34
GAPDH
MW(kDa)
1
2
C
Time (h)
0
8
64
51
p53-ub
p53
MW(kDa)
1 2 3 4 5
D
Nutlin-3
His-ubiquitin
His-pulldown
97
64
51
poly-Ub p53
mono-Ub p53
Unmodified p53
Direct Lysis
55
p53
95
72
MDM2
34
GAPDH
MW(kDa)
1 2 3
proteosome
?
E
DMSO
Nutlin
IR
His-ubiquitin
p53-Ub
97
64
51
Ub5
Ub2
Ub1
55
43
Unmodified p53
Direct Lysis
95
72
MDM2
34
p21
34
GAPDH
MW(kDa)
1 2 3 4 5
F
Fold increase (compared to respective control) AU
16
14
12
10
8
6
4
2
0
Nutlin
IR
unmodified
Ub1
Ub2
Ub5
G
Nutlin-3
Lactacystin
IR
Lactacystin
64
51
p53-ub
p53
MW (kDa)
1 2 3 4
Nutlin-3
IR
H
Time + cycloheximide (min)
0 15 30 60 90
control
Nutlin-3
IR
55
p53
MW(kDa)
p53 (% of protein remaining)
100
75
50
25
0
0 25 50 75 100
Time (min)
Nutlin-3
IR
control
I
Time + cycloheximide (min)
0 15 30 60 90
64
51
MW(kDa)
Control
Nutlin-3
IR
p53-ub
p53
High exposure

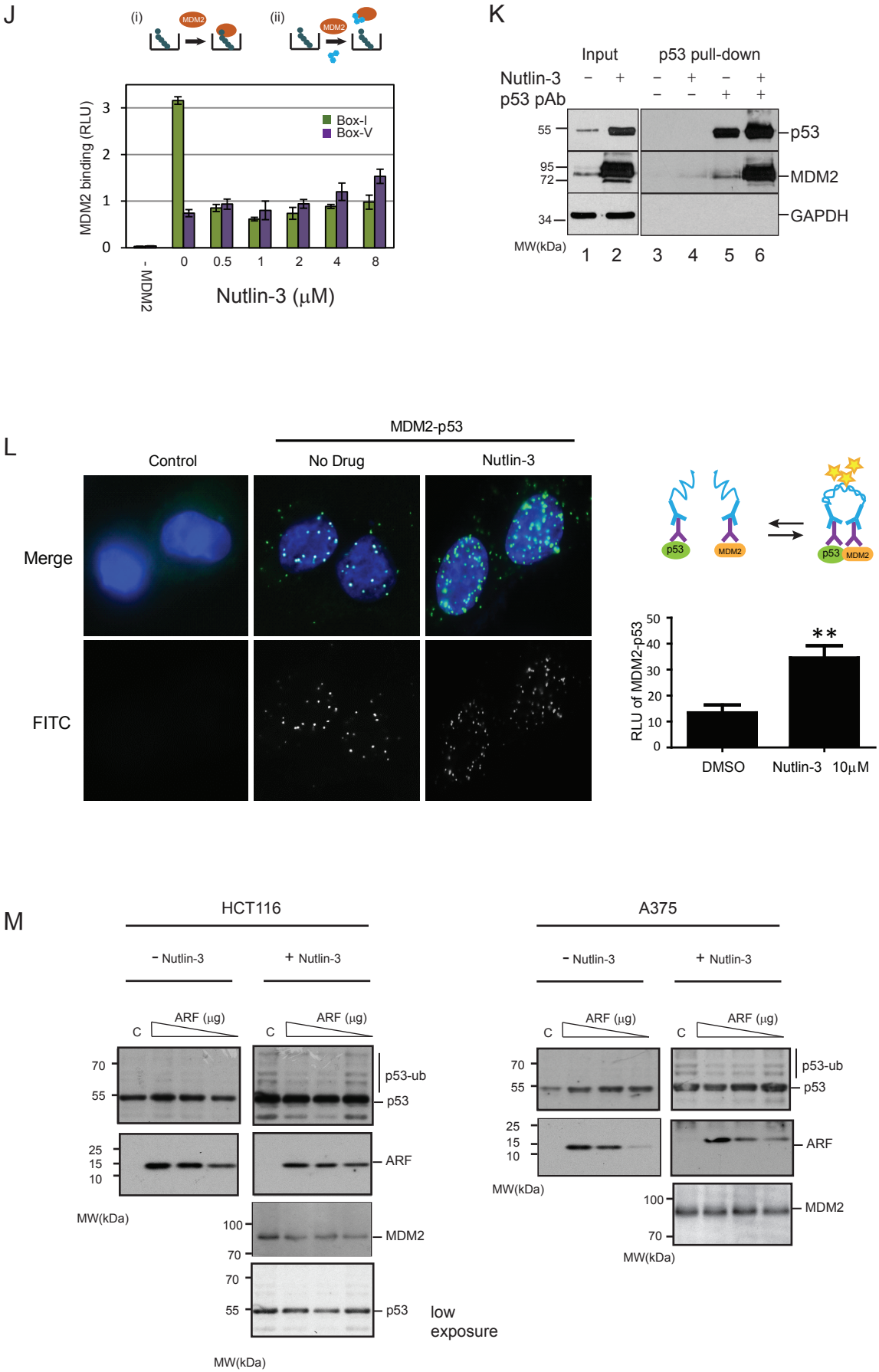
J
(i)
MDM2
(ii)
MDM2
MDM2 binding (RLU)
Box-I
Box-V
- MDM2
0
0.5
1
2
4
8
Nutlin-3 (μM)
K
Input
p53 pull-down
Nutlin-3
p53 pAb
p53
MDM2
GAPDH
MW(kDa)
1 2 3 4 5 6
L
MDM2-p53
Control
No Drug
Nutlin-3
Merge
FITC
p53
MDM2
RLU of MDM2-p53
DMSO
Nutlin-3 10μM
M
HCT116
A375
- Nutlin-3
+ Nutlin-3
ARF (μg)
C
p53-ub
p53
ARF
MDM2
MW(kDa)
low exposure

Figure 2

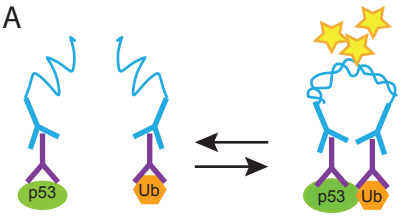
A
p53
Ub
p53
Ub

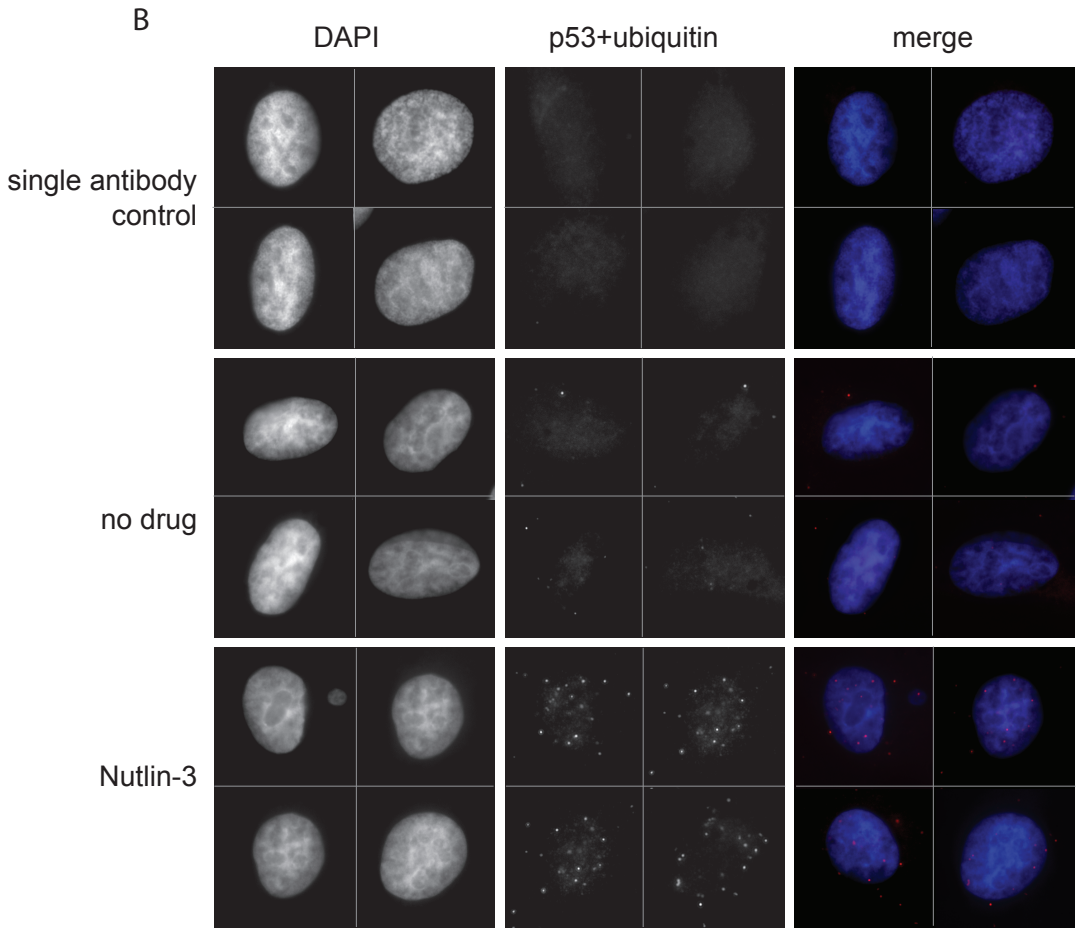
B
DAPI
p53+ubiquitin
merge
single antibody control
no drug
Nutlin-3

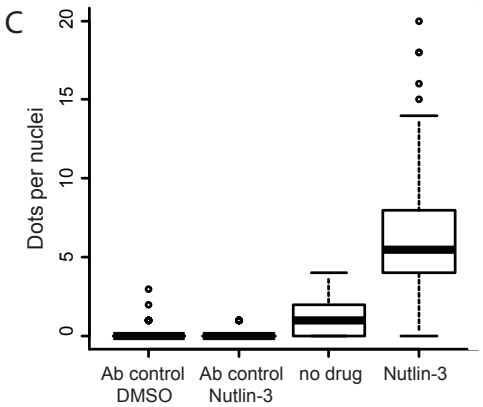
C
Dots per nuclei
0
5
10
15
20
Ab control DMSO
Ab control Nutlin-3
no drug
Nutlin-3

Figure 3

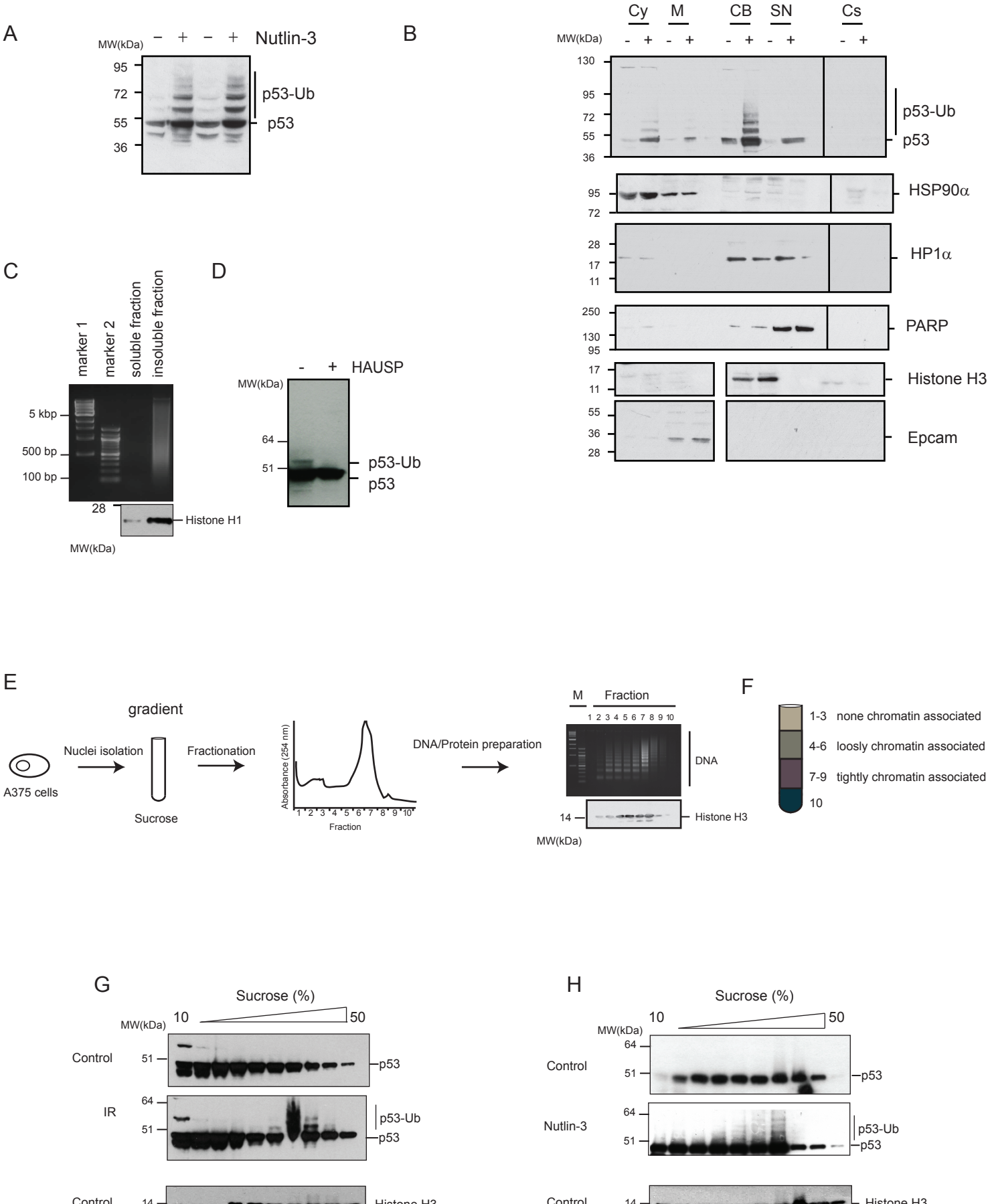
A
MW(kDa)
− + − + Nutlin-3
95
72
55
36
p53-Ub
p53
B
Cy M CB SN Cs
MW(kDa)
- + - + - + - + - +
130
95
72
55
36
p53-Ub
p53
95
72
HSP90α
28
17
11
HP1α
250
130
95
PARP
17
11
Histone H3
55
36
28
Epcam
C
marker 1
marker 2
soluble fraction
insoluble fraction
5 kbp
500 bp
100 bp
28
Histone H1
MW(kDa)
D
- + HAUSP
MW(kDa)
64
51
p53-Ub
p53
E
gradient
A375 cells
Nuclei isolation
Sucrose
Fractionation
Absorbance (254 nm)
1 2 3 4 5 6 7 8 9 10
Fraction
DNA/Protein preparation
M
Fraction
1 2 3 4 5 6 7 8 9 10
DNA
14
Histone H3
MW(kDa)
F
1-3 none chromatin associated
4-6 loosly chromatin associated
7-9 tightly chromatin associated
10
G
Sucrose (%)
MW(kDa)
10
50
Control
51
p53
IR
64
51
p53-Ub
p53
Control
14
Histone H3
Fraction: 1 2 3 4 5 6 7 8 9 10
H
Sucrose (%)
MW(kDa)
10
50
Control
64
51
p53
Nutlin-3
64
51
p53-Ub
p53
Control
14
Histone H3
Fraction: 1 2 3 4 5 6 7 8 9 10

Figure 4

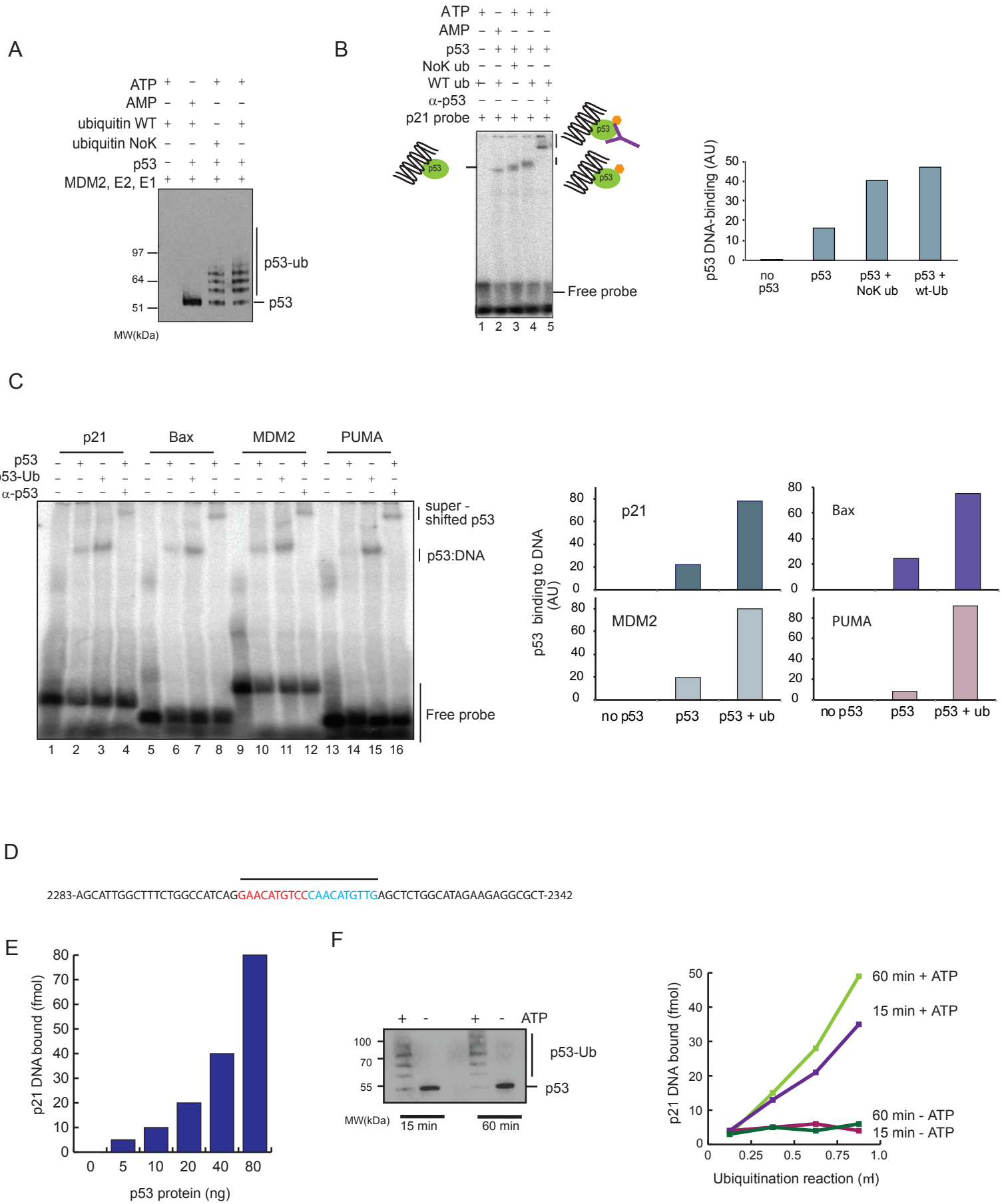
A
ATP
AMP
ubiquitin WT
ubiquitin NoK
p53
MDM2, E2, E1
97
64
51
p53-ub
p53
MW(kDa)
B
ATP
AMP
p53
NoK ub
WT ub
α-p53
p21 probe
p53
Free probe
1 2 3 4 5
p53 DNA-binding (AU)
no p53
p53
p53 + NoK ub
p53 + wt-Ub
C
p21
Bax
MDM2
PUMA
p53
p53-Ub
α-p53
super - shifted p53
p53:DNA
Free probe
1 2 3 4 5 6 7 8 9 10 11 12 13 14 15 16
p53 binding to DNA (AU)
no p53
p53
p53 + ub
D
2283-AGCATTGGCTTTCTGGCCATCAGGAACATGTCCCAACATGTTGAGCTCTGGCATAGAAGAGGCGCT-2342
E
p21 DNA bound (fmol)
p53 protein (ng)
F
ATP
p53-Ub
p53
MW(kDa)
15 min
60 min
60 min + ATP
15 min + ATP
60 min - ATP
15 min - ATP
p21 DNA bound (fmol)
Ubiquitination reaction (ml)

Figure 5

A

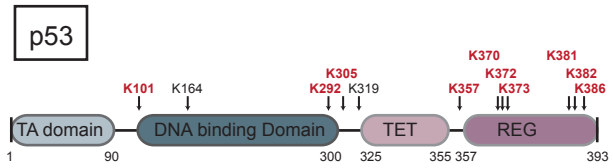
p53
K101
K164
K305
K292
K319
K370
K372
K373
K357
K381
K382
K386
TA domain
DNA binding Domain
TET
REG
1
90
300
325
355 357
393

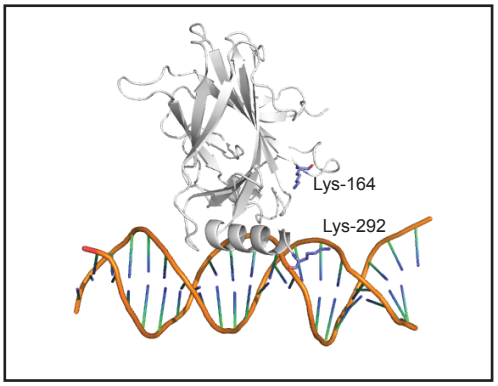
Lys-164
Lys-292

B

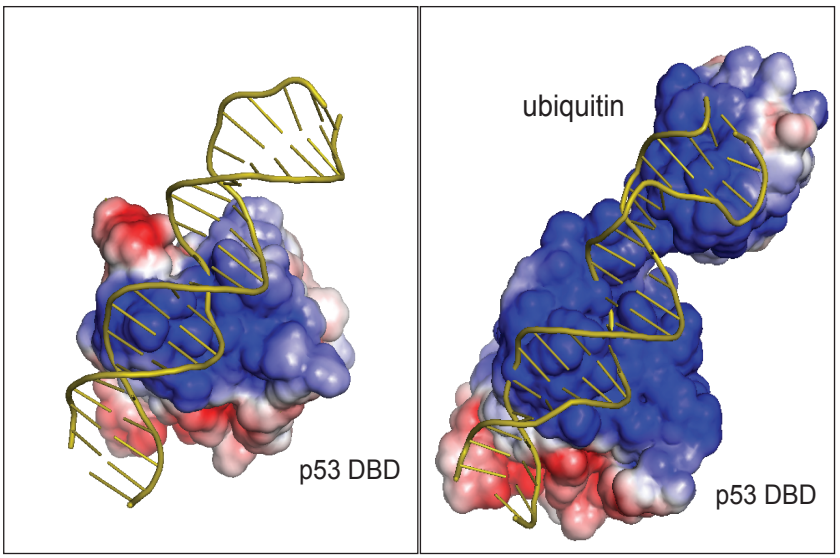
p53 DBD
ubiquitin
p53 DBD

C

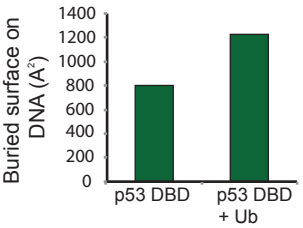
Buried surface on DNA (A²)
1400
1200
1000
800
600
400
200
0
p53 DBD
p53 DBD + Ub

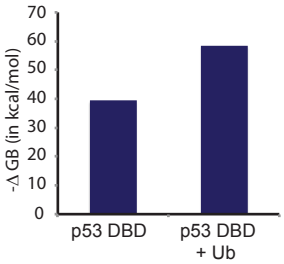
-Δ GB (in kcal/mol)
70
60
50
40
30
20
10
0
p53 DBD
p53 DBD + Ub

Figure 6

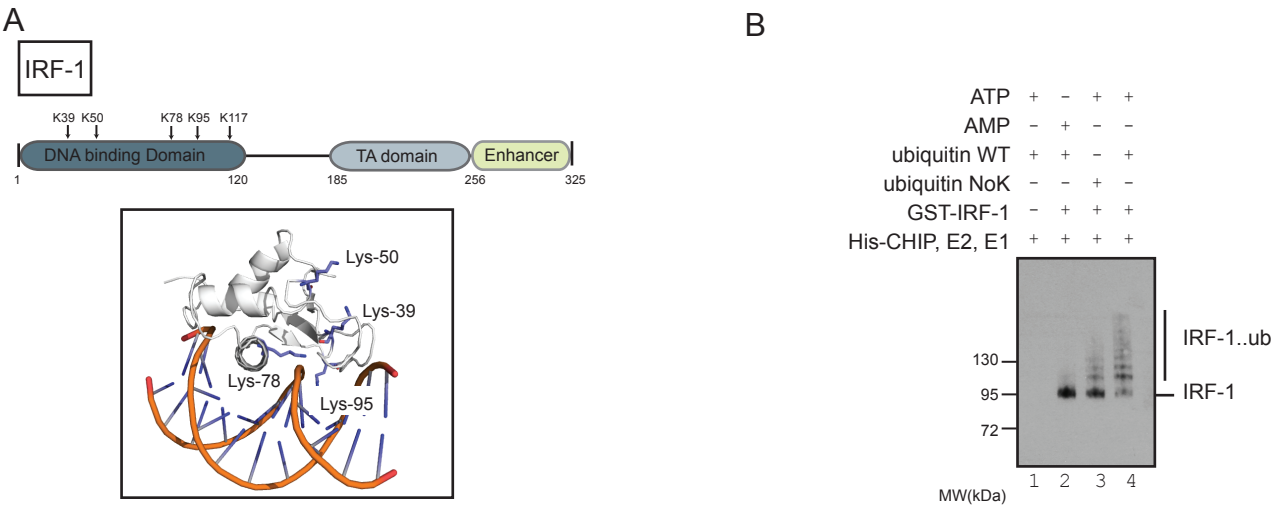
A
IRF-1
K39 K50
K78 K95 K117
DNA binding Domain
TA domain
Enhancer
1
120
185
256
325
Lys-50
Lys-39
Lys-78
Lys-95
B
ATP + − + +
AMP − + − −
ubiquitin WT + + − +
ubiquitin NoK − − + −
GST-IRF-1 − + + +
His-CHIP, E2, E1 + + + +
IRF-1..ub
IRF-1
130
95
72
1 2 3 4
MW(kDa)
C
ATP + − + +
AMP − + − −
IRF-1 − + + +
NoK ub − − + −
WT ub + + − +
C1 probe + + + +
IRF-1
NS
free probe
1 2 3 4
IRF-1 binding to DNA (AU)
60
40
20
0
no IRF-1
IRF-1
IRF-1 + NoK Ub
IRF-1 + WT Ub
D
unmodified
monoubiquitinated
polyubiquitinated
DNA-Binding (RLU)
20
15
10
5
0
0
10
20
30
40
IRF-1 (ng)
E
IRF-1 DBD
ubiquitin
IRF-1 DBD
F
Buried surface on DNA (A²)
2500
2000
1500
1000
500
0
IRF-1 DBD
IRF-1 DBD + Ub

Figure 7

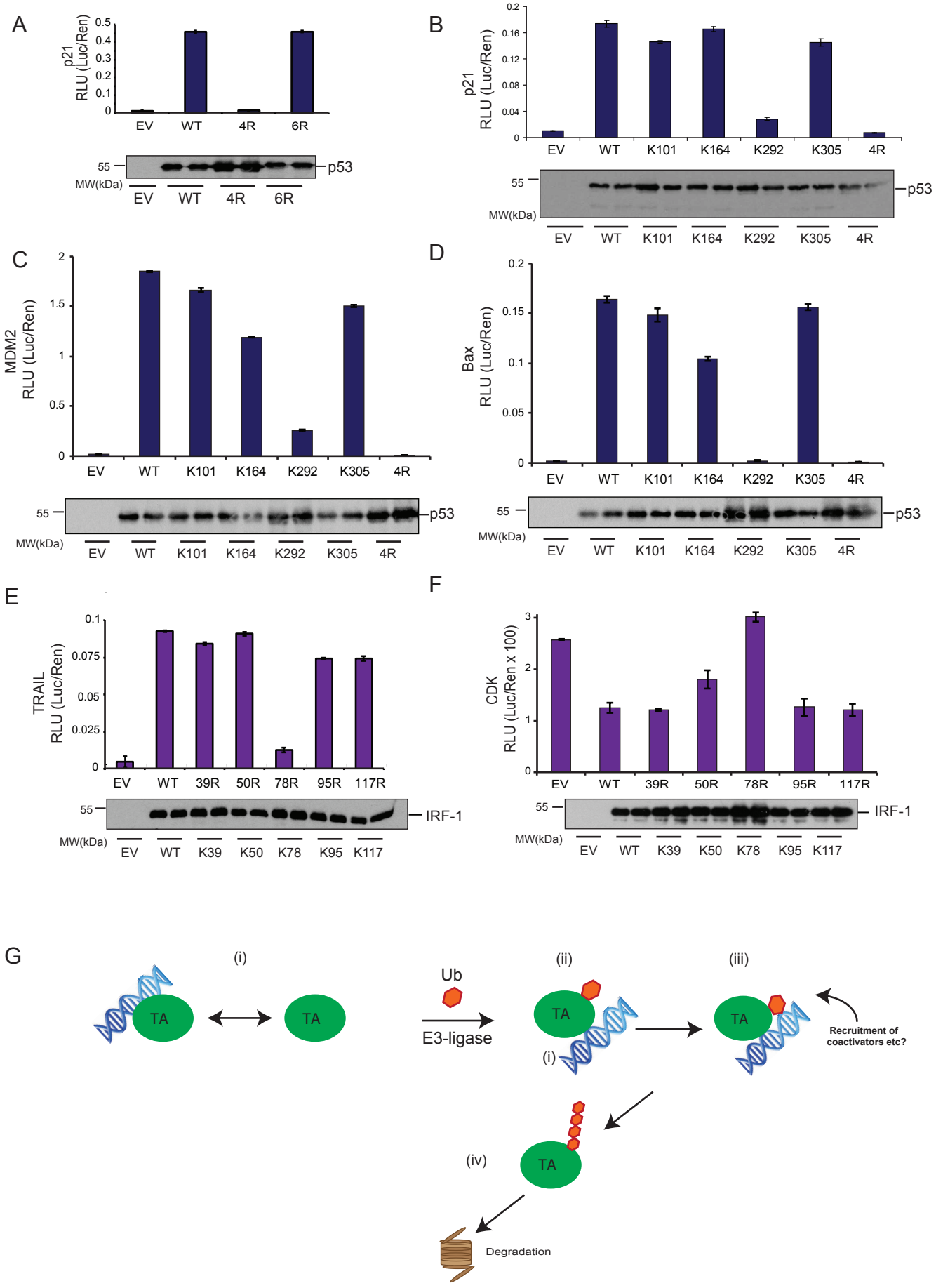
A
p21 RLU (Luc/Ren)
0.5
0.4
0.3
0.2
0.1
0
EV
WT
4R
6R
55
p53
MW(kDa)
EV
WT
4R
6R
B
p21 RLU (Luc/Ren)
0.2
0.16
0.12
0.08
0.04
0
EV
WT
K101
K164
K292
K305
4R
55
p53
MW(kDa)
EV
WT
K101
K164
K292
K305
4R
C
MDM2 RLU (Luc/Ren)
2
1.5
1
0.5
0
EV
WT
K101
K164
K292
K305
4R
55
p53
MW(kDa)
EV
WT
K101
K164
K292
K305
4R
D
Bax RLU (Luc/Ren)
0.2
0.15
0.1
0.05
0
EV
WT
K101
K164
K292
K305
4R
55
p53
MW(kDa)
EV
WT
K101
K164
K292
K305
4R
E
TRAIL RLU (Luc/Ren)
0.1
0.075
0.05
0.025
0
EV
WT
39R
50R
78R
95R
117R
55
IRF-1
MW(kDa)
EV
WT
K39
K50
K78
K95
K117
F
CDK RLU (Luc/Ren x 100)
3
2
1
0
EV
WT
39R
50R
78R
95R
117R
55
IRF-1
MW(kDa)
EV
WT
K39
K50
K78
K95
K117
G
(i)
TA
TA
Ub
E3-ligase
(ii)
TA
(i)
(iii)
TA
Recruitment of coactivators etc?
(iv)
TA
Degradation